

Experimental test of nonclassicality for a single particle

Giorgio Brida¹, Ivo Pietro Degiovanni^{1*}, Marco Genovese¹, Valentina Schettini¹, Sergey V. Polyakov² and Alan Migdall²

¹Istituto Nazionale di Ricerca Metrologica, Strada delle Cacce 91, 10135 Torino, Italy

²Optical Technology Division, National Institute of Standards and Technology, 100 Bureau Drive, Gaithersburg, MD 20899-8441 and Joint Quantum Institute, Univ. of Maryland, College Park, MD 20742

*Corresponding author: i.degiovanni@inrim.it

Abstract: In a recent paper [R. Alicki and N. Van Ryn, J. Phys. A: Math. Theor., **41**, 062001 (2008)] a test of nonclassicality for a single qubit was proposed. Here, we discuss the class of hidden variables theories to which this test applies and present an experimental realization.

© 2008 Optical Society of America

OCIS codes: (270.0270) Quantum optics; (270.5585) Quantum information and processing

References and links

1. A. Einstein, B. Podolsky, and N. Rosen, "Can quantum-mechanical description of physical reality be considered complete?", *Phys. Rev.* **47**, 777-780 (1935).
2. J. S. Bell, "On the Einstein Podolsky Rosen paradox," *Physics* **1**, 195-200 (1964).
3. M. Genovese, "Research on hidden variable theories: A review of recent progresses," *Phys. Rep.* **413**, 319-396 (2005).
4. A. Aspect, J. Dalibard, and G. Roger, "Experimental Test of Bell's Inequalities Using Time-Varying Analyzers," *Phys. Rev. Lett.* **49**, 1804-1807 (1982).
5. J. P. Franson, "Bell inequality for position and time," *Phys. Rev. Lett.* **62**, 2205-2208 (1989).
6. J. G. Rarity and P. R. Tapster, "Experimental violation of Bells inequality based on phase and momentum," *Phys. Rev. Lett.* **64**, 2495-2498 (1990).
7. J. Brendel, E. Mohler, and W. Martienssen, "Experimental Test of Bell's Inequality for Energy and Time," *Eur. Phys. Lett.* **20**, 575-580 (1993).
8. P. G. Kwiat, W. A. Vareka, C. K. Hong, H. Nathel, and R. Y. Chiao, "Correlated two-photon interference in a dual-beam Michelson interferometer," *Phys. Rev. A* **41**, 2910-2913 (1990).
9. T. E. Kiess, Y. H. Shih, A. V. Sergienko, and C. O. Alley, "Einstein-Podolsky-Rosen-Bohm experiment using pairs of light quanta produced by type-II parametric down-conversion," *Phys. Rev. Lett.* **71**, 3893-3897 (1993).
10. P. G. Kwiat, K. Mattle, H. Weinfurter, A. Zeilinger, A. V. Sergienko, and Y. Shih, "New High-Intensity Source of Polarization-Entangled Photon Pairs," *Phys. Rev. Lett.* **75**, 4337-4341 (1995).
11. Z. J. Ou and L. Mandel, "Violation of Bell's Inequality and Classical Probability in a Two-Photon Correlation Experiment," *Phys. Rev. Lett.* **61**, 50-53 (1988).
12. Y. H. Shih, A. V. Sergienko, and M. H. Rubin, "Einstein-Podolsky-Rosen state for space-time variables in a two-photon interference experiment," *Phys. Rev. A* **47**, 1288-1293 (1993).
13. J. R. Torgerson, D. Branning, C. H. Monken, and L. Mandel, "Experimental demonstration of the violation of local realism without Bell inequalities," *Phys. Lett. A* **204**, 323-328 (1995).
14. J.-W. Pan, D. Bouwmeester, M. Daniell, H. Weinfurter and A. Zeilinger, "Experimental test of quantum nonlocality in three-photon Greenberger-Horne-Zeilinger entanglement," *Nature* **403**, 515-519 (2000).
15. G. Brida, M. Genovese, C. Novero, and E. Predazzi, "New experimental test of Bell inequalities by the use of a non-maximally entangled photon state," *Phys. Lett. A* **268**, 12-16 (2000).
16. W. Tittel, J. Brendel, H. Zbinden, and N. Gisin, "Violation of Bell Inequalities by Photons More Than 10 km Apart," *Phys. Rev. Lett.* **81**, 3563-3566 (1998).
17. G. Weihs, T. Jennewein, C. Simon, H. Weinfurter, and A. Zeilinger, "Violation of Bell's Inequality under Strict Einstein Locality Conditions," *Phys. Rev. Lett.* **81**, 5039-5043 (1998).
18. M. A. Rowe, D. Kielpinski, V. Meyer, C. A. Scakett, W. M. Itano, C. Monroe, and D. J. Wineland, "Experimental violation of a Bell's inequality with efficient detection," *Nature* **409**, 791-794 (2001).

19. S. Groblacher, T. Paterek, R. Kaltenbaek, C. Brukner, M. Zukowski, M. Aspelmeyer, and A. Zeilinger, "An experimental test of non-local realism," *Nature* **446**, 871-875 (2007).
20. C. Branciard, A. Ling, N. Gisin, C. Kurtsiefer, A. Lamas-Linares, and V. Scarani, "Experimental Falsification of Leggett's Nonlocal Variable Model," *Phys. Rev. Lett.* **99**, 210407 (2007).
21. T. Paterek, A. Fedrizzi, S. Groblacher, T. Jennewein, M. Zukowski, M. Aspelmeyer, and A. Zeilinger, "Experimental Test of Nonlocal Realistic Theories Without the Rotational Symmetry Assumption," *Phys. Rev. Lett.* **99**, 210406 (2007).
22. G. Brida, M. Genovese, C. Novero, and E. Predazzi, "A first test of Wigner function local realistic model," *Phys. Lett. A* **299**, 121-124 (2002).
23. G. Brida, M. Genovese, and F. Piacentini, "Experimental local realism tests without fair sampling assumption," *Eur. Phys. J. D* **44**, 577-580 (2007).
24. G. Brida, E. Cagliero, G. Falzetta, M. Genovese, M. Gramegna and C. Novero, "Experimental realization of a first test of de Broglie-Bohm theory," *J. Phys. B: At. Mol. Opt. Phys.*, **35**, 4751-4756 (2002).
25. G. Brida, E. Cagliero, G. Falzetta, M. Genovese, M. Gramegna, and E. Predazzi, "Biphoton double-slit experiment," *Phys. Rev. A* **68**, 033803 (2003).
26. M. D. Eisaman, E. A. Goldschmidt, J. Chen, J. Fan, and A. Migdall, "Experimental test of nonlocal realism using a fiber-based source of polarization-entangled photon pairs," *Phys. Rev. A* **77**, 032339 (2008).
27. A. Leggett, "Nonlocal Hidden-Variable Theories and Quantum Mechanics: An Incompatibility Theorem," *Found. Phys.* **33**, 1469-1493 (2003).
28. G. Auletta, *Foundations and Interpretation of Quantum Mechanics* (World Scientific, Singapore, 2000).
29. R. Alicki and N. Van Ryn, "A simple test of quantumness for a single system," *J. Phys. A: Math. Theor.*, **41**, 062001 (2008).
30. F. De Zela, "Single-qubit tests of Bell-like inequalities," *Phys. Rev. A* **76**, 042119 (2007).
31. R. Lapiedra, "Joint reality and Bell inequalities for consecutive measurements," *Eur. Phys. Lett.* **75**, 202-208 (2006).
32. R. Ruskov, A. N. Korotkov, and A. Mizel, "Signatures of Quantum Behavior in Single-Qubit Weak Measurements," *Phys. Rev. Lett.* **96**, 200404 (2006).
33. A. N. Jordan, A. N. Korotkov, and M. Bittiker, "Leggett-Garg Inequality with a Kicked Quantum Pump," *Phys. Rev. Lett.* **97**, 026805 (2006).
34. J. D. Malley, A. Fine, "Noncommuting observables and local realism," *Phys. Lett. A* **347**, 51 (2005).
35. This follows from C^* -algebra theory as well as [29].
36. A study to fully identify such a class and possibility of its expansion via additional measurements is underway.
37. S. Castelletto, I. P. Degiovanni, V. Schettini, and A. Migdall, "Optimizing single-photon-source heralding efficiency and detection efficiency metrology at 1550 nm using periodically poled lithium niobate," *Metrologia* **43**, S56-S60 (2006).
38. V. Schettini, S. V. Polyakov, I. P. Degiovanni, G. Brida, S. Castelletto, and A. L. Migdall, "Implementing a Multiplexed System of Detectors for Higher Photon Counting Rates," *IEEE J. Sel. Top. Quantum Electron.* **13**, 978-983 (2007).
39. We note that while this test could have been setup using a more conventional component for the variable beam-splitter than the optical switch, it was used in this case because it served the purpose and was already in place from an earlier experiment.
40. P. Grangier, G. Roger, and A. Aspect, "Experimental evidence for a photon anticorrelation effect on a beam splitter: a new light on single-photon interferences," *Europhys. Lett.* **11**, 173-179 (1986).

1. Introduction

The quest for a classical theory able to reproduce the results of Quantum Mechanics (QM) has a pluridecennial history, stemming from the 1935 Einstein-Podolsky-Rosen paper [1], where the completeness of QM was questioned.

In 1964 Bell showed that for some hidden variable theories (HVTs), specifically, for every local realistic theory (LRT) [2], correlations among certain observables measured on entangled states must satisfy a set of inequalities (the Bell's inequalities, BI), while for QM they can be violated, with many experiments [3, 4, 5, 6, 7, 8, 9, 10, 11, 12, 13, 14, 15, 16, 17, 18] showing violation of BI's. In the last decade the study of QM vs. LRT for certain realistic models [3, 19, 20, 21, 22, 23, 24, 25, 26, 27] has attracted new interest fueled by the development of Quantum Information science [3]. We note that, some classes of LRTs have not been excluded by Bell's inequality experiments because of experimentally induced loophole(s). Experiments specifically aimed at testing those LRTs are the focus of recent interest. Other differences be-

tween quantum and classical treatments have also been discovered and pointed out [28].

Recently, a test of nonclassicality at the single qubit level was proposed [29]. This test is very appealing both because of its simplicity (particularly in comparison with other proposals to test nonclassicality at a single qubit level [30, 31, 32, 33, 34]) and its ability to show that some quantum states in a two dimensional Hilbert space cannot be classical. We note that because this is a test of single particle states, there is no reference made to the question of locality, rather it is a more fundamental test of nonclassicality with respect to possibility of an underlying hidden variable theory. It does, however, allow testing of specific classes of states (i.e. those with observables satisfying certain “classical” properties discussed later), although like the Bell test, it is subject to a number of loopholes depending on its experimental implementation. The purpose of this work is twofold: first, we want to start a discussion on the advantages and limitations of this new proposal, and second, we present the first experimental implementation of this test, which we have realized with a conditional single-photon source.

2. Theoretical Model

The proposal, [29], is based on the fact that given any two positive real functions \mathcal{A}, \mathcal{B} obeying the relation

$$0 \leq \mathcal{A}(x) \leq \mathcal{B}(x) \quad (1)$$

that for any probability distribution $\rho(x)$ it must be true that

$$\langle \mathcal{A}^2 \rangle \equiv \int \mathcal{A}^2(x) \rho(x) dx \leq \int \mathcal{B}^2(x) \rho(x) dx \equiv \langle \mathcal{B}^2 \rangle. \quad (2)$$

For quantum systems, one can find pairs of observables \hat{A}, \hat{B} such that the minimum eigenvalue of $\hat{B} - \hat{A}$ is greater than zero which we refer to as the the inequality

$$0 \leq \hat{A} \leq \hat{B}. \quad (3)$$

The commutation relations stemming from the classical approach that lead to Eq. (2), prescribe that for all systems (described by the density matrix $\hat{\rho}$)

$$\langle \hat{A}^2 \rangle \leq \langle \hat{B}^2 \rangle, \quad (4)$$

where $\langle \hat{O} \rangle \equiv \text{Tr}[\hat{O} \hat{\rho}]$, while on the contrary, quantum theory allows that for certain quantum states

$$\langle \hat{A}^2 \rangle > \langle \hat{B}^2 \rangle. \quad (5)$$

This sharp difference between classical (in the sense discussed above) and quantum theory predictions at a single qubit level [35] can be tested experimentally on an ensemble of single particles. In this paper we experimentally apply this method to single-photons using the polarization degree of freedom, as suggested in Ref. [29]. We do note that because, by definition, hidden variables (such as may be represented by x above) cannot be observed directly, the condition given in Eq. (1) defines and limits the class of hidden variable theories that can be tested by violation of the “classical” inequality (2) [36].

Quantum objects used to implement this test are horizontally polarized single-photons ($|H\rangle$) produced by a heralded single-photon source. Our two observables are

$$\hat{A} = a_0 \hat{P}_\alpha \quad (6)$$

and

$$\hat{B} = b_0 \left[p_1 \hat{P}_\beta + (1 - p_1) \hat{P}_{\beta+\pi/2} \right], \quad (7)$$

with numerical constants a_0 and b_0 , \hat{P}_θ is the projector on the state $|s(\theta)\rangle = \cos \theta |H\rangle + \sin \theta |V\rangle$ (and $\hat{P}_{\theta+\pi/2}$ is the projector on the orthogonal state $\sin \theta |H\rangle - \cos \theta |V\rangle$), and $0 \leq p_1 \leq 1$.

The expectation value $\langle \hat{A} \rangle$ can be obtained experimentally by projecting heralded photons onto the state $|s(\alpha)\rangle$, while $\langle \hat{B} \rangle$ is realized with an experimental setup that projects heralded photons onto the state $|s(\beta)\rangle$ with probability p_1 , and onto the state $|s(\beta + \pi/2)\rangle$ with probability $(1 - p_1)$. This probabilistic projection can be achieved, in principle, with a beam-splitter with a splitting ratio p_1 , sending photons towards the two projection systems.

The experimental measurement of both $\langle \hat{A} \rangle$ and $\langle \hat{A}^2 \rangle$, where $\hat{A}^2 = a_0^2 \hat{P}_\alpha$, is achieved by projecting the photon onto the state $|s(\alpha)\rangle$. To measure $\langle \hat{B}^2 \rangle$, where $\hat{B}^2 = b_0^2 [p_1^2 \hat{P}_\beta + (1 - p_1)^2 \hat{P}_{\beta+\pi/2}]$, however, it is necessary to change the beam splitting ratio to $p_2 = \frac{p_1^2}{p_1^2 + (1 - p_1)^2}$. Thus the operator \hat{B}^2 is:

$$\hat{B}^2 = b_0^2 \frac{1 - 2\sqrt{(1 - p_2)p_2}}{(1 - 2p_2)^2} [p_2 \hat{P}_\beta + (1 - p_2) \hat{P}_{\beta+\pi/2}], \quad (8)$$

in terms of the splitting ratio p_2 . We assume that the beamsplitter randomly and fairly splits the incoming photons, with the probabilities that are equivalent to the splitting ratio of “classical” waves.

It can be shown that for the parameters set to $a_0 = 0.74$, $b_0 = 1.2987$, $p_1 = 4/5$, $p_2 = 16/17$, $\alpha = 11/36 \pi$, and $\beta = 5/12 \pi$, the results predicted by quantum theory are $\langle \hat{B}^2 \rangle - \langle \hat{A}^2 \rangle = -0.0449$, and $\langle \hat{B} \rangle - \langle \hat{A} \rangle = 0.0685$, while the minimum eigenvalue of $\hat{B} - \hat{A}$ is $d_- = 0.0189$, where

$$d_- \equiv \frac{1}{2} \left\{ b_0 - a_0 - \sqrt{a_0^2 + b_0^2 (1 - 2p_1)^2 + 2 a_0 b_0 (1 - 2p_1) \cos[2(\alpha - \beta)]} \right\}. \quad (9)$$

We note that the value of d_- obtainable with the parameters suggested in Ref. [29] is 0.00057, too close to zero to ensure the positivity of $\hat{B} - \hat{A}$ in our experimental measurement. For this reason we chose the above set of parameters leading to a value for d_- almost two orders of magnitude larger.

The critical question is whether the above arrangement can serve as a test of all HVTs. As mentioned in the discussion of Eqs. (1)-(5), the test proposed in Ref. [29] concerns the class of HVTs satisfying Eq. (1) only. The simplest example of a HVT that does not satisfy this condition and can mimic QM, relies on a hidden (or simply unmeasured) variable x uniformly distributed between 0 and 1 ($\rho(x) = 1$ when $0 \leq x \leq 1$), and classical quantities $\mathcal{A}(x) = a_0 \theta(X_A - x)$, and $\mathcal{B}(x) = b_0 [p_1 \theta(X_B - x) + (1 - p_1) \theta(x - X_B)]$, where $\theta(\xi)$ is the step function (1 for $\xi \geq 0$, and 0 elsewhere). By choosing $X_A = \cos^2 \alpha$ and $X_B = \cos^2 \beta$ and using the experimental parameters defined above, we obtain the quantum mechanical predictions, $\langle \mathcal{B} \rangle - \langle \mathcal{A} \rangle = 0.0685$ and $\langle \mathcal{B}^2 \rangle - \langle \mathcal{A}^2 \rangle = -0.0449$. It is easy to verify that this model does not belong to the class of hidden variable models falsified by this test, as the condition given in Eq. (1) is not satisfied for some x . In particular, for $X_B < x < X_A$ we have $\mathcal{A}(x) > \mathcal{B}(x)$. The boundary of the class of HVTs identified by condition (1), as well as the possibility of enlarging the class by modifying this method is a very important question, but is beyond the scope of this work.

3. Experiment

The experimental setup is presented in Fig. 1. The heralded single-photon source is based on photon pairs produced by parametric down conversion (PDC). Our PDC source is a 5 mm long periodically poled MgO-doped lithium niobate (PPLN) crystal, pumped by a continuous wave (cw) laser at 532 nm, that produces pairs of correlated photons at 810 nm and 1550 nm [37]. A

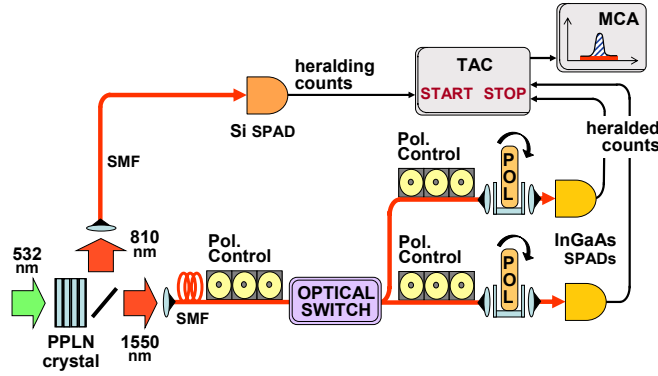


Fig. 1. Experimental setup. A PDC heralded single-photon source generates pairs of photons at 810 nm (heralding) and 1550 nm (heralded) in a PPLN crystal pumped by a 532 nm laser. The heralded photons are sent to the measurement apparatus designed to evaluate the observables $\langle \hat{A} \rangle$, $\langle \hat{A}^2 \rangle$, $\langle \hat{B} \rangle$, and $\langle \hat{B}^2 \rangle$.

cutoff filter blocks the pump laser light at the crystal's output and a dichroic mirror separates the 810 nm and 1550 nm photons. Extra interference filters at 810 and 1550 nm with a full width half-maximums (FWHM) of 10 nm and 30 nm, respectively, further suppress fluorescence from the PPLN crystal reducing background counts. The collection geometry on the heralding arm restricts the visible bandwidth to ≈ 2 nm FWHM.

The heralded single-photon source is independently characterized to ensure that a) there is a sizable correlation between the signal photons at 810 and 1550 nm that dominates over the background of accidental coincidences and b) that multiphoton emission is negligible (i.e. when conditioned on a photon detection at 810 nm, the probability to observe two photons in a 1550 path is negligible, see Appendix.)

For the experiment, photons in the heralding arm are routed by a single-mode fiber (SMF) to a Si-single-photon Avalanche Diode (SPAD) operating in Geiger mode, while photons in the heralded arm, coupled into a second SMF, are sent to the apparatus that implements the probabilistic projections according to the parameter values determined above (necessary to measure $\langle \hat{B} \rangle$ and $\langle \hat{B}^2 \rangle$). These projections are implemented by means of an all-fiber variable beam splitter and polarizers.

The variable beam-splitter is made from an optical switch that can route heralded photons with an adjustable splitting ratio into two different optical paths [38]. The input polarization state in each optical path after the beamsplitter is controlled using a three paddle single-mode fiber polarization rotator followed by a rotating polarizer (POL).

This scheme allows us to set the polarizers to perform projections on \hat{P}_α , \hat{P}_β , and $\hat{P}_{\beta+\pi/2}$, and set the splitting probability of the beam splitter to p_1 or p_2 to make necessary measurements of the observables [39]. After passing through the polarizers that performed the projections, the heralded photons were finally sent to InGaAs-SPADs gated by the Si-SPAD heralding counts.

We determine the true coincidence probability for each gate, rather than using the raw measured counts to eliminate the contribution of accidental coincidences, detector deadtimes, and drifts. The probability for each measurement i was evaluated according to

$$\eta_i(\theta, p) = \frac{N_i(\theta, p)}{M_{g,i}}, \quad (10)$$

where $N_i(\theta, p)$ is the number of coincidences sent with probability p towards the detection system with the polarizer projecting photons onto the state $|s(\theta)\rangle$, and $M_{g,i}$ is the number of heralding gate counts. Thus, in each experimental configuration, $\langle \hat{P}(\theta) \rangle$ was estimated as

$$\mathcal{E}[\langle \hat{P}(\theta) \rangle] = \frac{\sum_i \eta_i(\theta, p)}{\sum_i [\eta_i(\theta, p) + \eta_i(\theta + \pi/2, p)]}, \quad (11)$$

while the probability of sending a photon towards a detection system (whose nominal value is p) was estimated as

$$\mathcal{E}[p] = \frac{\sum_i [\eta_i(\theta, p) + \eta_i(\theta + \pi/2, p)]}{\sum_i \left[\eta_i(\theta, p) + \eta_i(\theta, 1-p) + \eta_i(\theta + \pi/2, p) + \eta_i(\theta + \pi/2, 1-p) \right]}. \quad (12)$$

Quantity	Measurement	QM theory
$\mathcal{E}[\langle \hat{B} \rangle - \langle \hat{A} \rangle]$	$0.0581 \pm 0.0049 (\pm 0.0112)$	0.0685
$\mathcal{E}[\langle \hat{B}^2 \rangle - \langle \hat{A}^2 \rangle]$	$-0.0403 \pm 0.0043 (\pm 0.0066)$	-0.0449 (> 0 HVTs)
$\mathcal{E}[p_1]$	0.80 ± 0.01	0.800
$\mathcal{E}[p_2]$	0.94 ± 0.01	0.941

Table 1. Measurement results with statistical and total uncertainties and theoretical predictions. The total uncertainty (in parentheses) accounts for both statistical and systematic effects.

Using Eqs. (11) and (12) we computed the experimental values of $\langle \hat{A} \rangle$, $\langle \hat{A}^2 \rangle$, $\langle \hat{B} \rangle$, and $\langle \hat{B}^2 \rangle$ as seen in Table 1. From the same experimental results we obtained an indirect evaluation of the minimum eigenvalue of $\hat{B} - \hat{A}$ as (0.0101 ± 0.0065) , showing that we have met requirement (3) (we point out that the high relative uncertainty of this evaluation is due to its indirect determination). From the value of $\mathcal{E}[\langle \hat{B}^2 \rangle - \langle \hat{A}^2 \rangle]$ we show a violation of the classical limit (Eq. (4)) by more than 6 standard deviations.

Table 1 presents both the statistical and total uncertainties. Statistical uncertainties include those due to Poisson counting statistics as well as those due to random misalignment of the polarizers (we estimate an angular uncertainty of 2.5°), while the total uncertainties also include systematic effects such as the uncertainty in setting the optical switch voltage bias used to obtain the required splitting ratio. As an additional test, we measured $\mathcal{E}[p_1]$ and $\mathcal{E}[p_2]$ and found them consistent with the intended settings (see Table 1). Furthermore, we analyzed how the non-ideal (multi-photon) behavior of our single-photon source might have affected the experimental results, and we found its effects to be negligible, being more than an order magnitude below the listed uncertainties.

4. Conclusions

In conclusion, we have investigated the theoretical proposal for testing nonclassicality of a single-particle state [29]. While the utility of this test is open to question, as it does not apply to every conceivable HVT like Bells inequalities, but only the class of HVTs satisfying Eq. (1), we have nonetheless experimentally implemented it as proposed. Following the test's protocol, our measurement results are seen to be incompatible with a certain class of HVTs (as defined by Eq. (1)) while being well predicted by QM. In particular, our results clearly falsify this HVT class by 6 standard deviations. The precise identification of this class and whether and if it maps to any physical system remains to be determined. Also to be determined is whether it is possible to extend or generalize this test to cover a larger class of HVTs. This effort represents a first step in this direction of providing a sharp difference between QM and HVTs at the single qubit level/two dimensional Hilbert space and a physical implementation of that test.

Appendix

A necessary requirement for a convincingly realizing the Alicki-Van Ryn's proposal [29] is a demonstration that our source in fact produces single-photon states.

First, we verify that the source optics are aligned to collect correlated photons. The correlation between the two arms of the source is measured with a Time to Amplitude Converter (TAC) and a Multi-Channel Analyzer (MCA). The MCA output (Fig. 2) shows the correlation peak along with the background of uniformly distributed accidental counts, as expected for our photon source. (We used a gate time of ≈ 20 ns for the InGaAs-SPAD.) From this shape, we can subtract the background (i.e. counts not produced by photons of the same pair) from signal, or true coincidences (i.e. the simultaneous generation of a heralded photon and its heralding twin).

Second, we verify that the possibility of having more than one photon in the heralded arm after detecting the heralding photon is low. With this aim we use the same setup as for the main experiment (Fig. 1), but with the polarizers removed and the splitting factor of the switch set to $p = (0.50 \pm 0.01)$. The efficiency of a single-photon source can be described by means of the two parameters $\Gamma_1 = Q(1)/Q(0)$ and $\Gamma_2 = Q(2)/Q(1)$, where $Q(0)$ is the probability that for each heralding count neither InGaAs-SPAD in the heralded arm fires, $Q(1)$ is the probability of detecting just one count for each herald, and $Q(2)$ is the probability of observing a coincidence for each heralding count from simultaneous firings by the two InGaAs-SPADs.

In general, a heralding detection announces the arrival of a “pulse” containing n photons at the heralded channel. The probability of a specific InGaAs-SPAD firing due to a heralded optical pulse containing n photons is

$$\begin{aligned} Q(1|n) &= \sum_{m=0}^n [1 - (1 - \tau)^m] B(m|n; p) = \\ &= 1 - (1 - p \tau)^n, \end{aligned} \quad (13)$$

where p is the optical switch splitting ratio, $B(m|n; p) = n!/[m!(n-m)!]^{-1} p^m (1-p)^{n-m}$ is the binomial distribution representing the splitting of n photons towards the two InGaAs-SPADs, and τ is the detection efficiency of each InGaAs-SPAD (that also accounts for all collection and optical losses in the channel). Analogously, the probability of observing a coincidence between the two InGaAs-SPADs due to a heralded optical pulse with n photons is

$$\begin{aligned} Q(2|n) &= \sum_{m=0}^n [1 - (1 - \tau)^m][1 - (1 - \tau)^{n-m}] B(m|n; p) \\ &= 1 - (1 - p \tau)^n - [1 - (1 - p \tau)]^n + (1 - \tau)^n. \end{aligned} \quad (14)$$

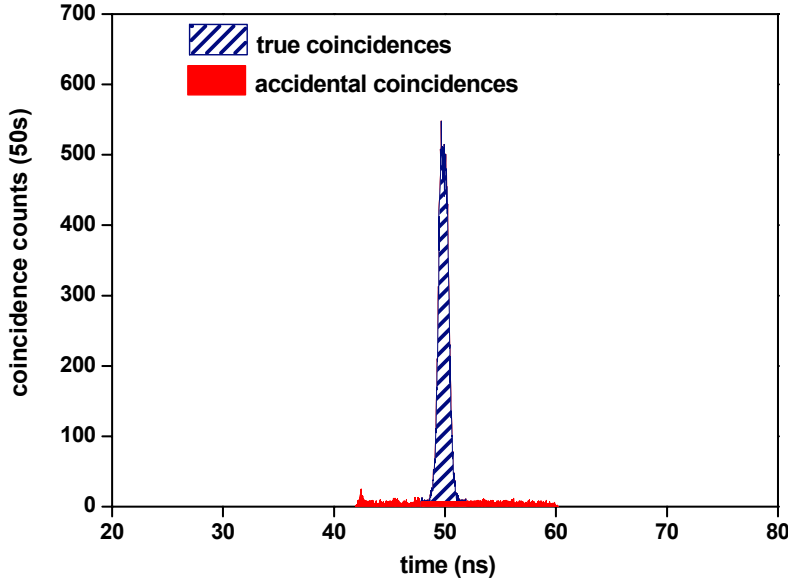


Fig. 2. Typical correlation between the detection of heralding and heralded photons, showing the coincidences peak due to heralded counts (true coincidences) and the uniformly distributed accidental coincidences. InGaAs-SPAD gate time was approximately 20 ns.

Thus we get $Q(1) = \sum_n Q(1|n)\mathcal{P}(n)$, and $Q(2) = \sum_n Q(2|n)\mathcal{P}(n)$ for $\mathcal{P}(n)$ being the general probability distribution of the number of photons in a heralded optical pulse. Setting $p = 0.5$, in the case of an ideal single-photon source ($\mathcal{P}(n) = \delta_{n,1}$) we obtain $Q(1) = \tau/2$, and $Q(2) = 0$, corresponding to $\Gamma_2 = 0$ and $\Gamma_1 = \tau/[2(1 - \tau/2)]$; while for a Poissonian source ($\mathcal{P}(n) = {}^n e^{-\tau} / n!$) we obtain $Q(1) = 1 - \exp(-\tau/2)$, and $Q(2) = [1 - \exp(-\tau/2)]^2$, corresponding to $\Gamma_2 = 1 - \exp(-\tau/2)$ and $\Gamma_1 = \exp(\tau/2) - 1$ (meaning $\Gamma_2 \simeq \Gamma_1 = \tau/2$ when $\tau \ll 1$). See Table 2 for comparison between the ideal sources above and our implementation.

Source Type	Γ_1	Γ_2	Γ_2/Γ_1
Single-photon	$\tau/[2(1 - \tau/2)]$	0	0
Poisson	$e^{\tau/2} - 1$	$1 - e^{-\tau/2}$	≈ 1 (when $\tau \ll 1$)
This	$(4.14 \pm 0.06) \cdot 10^{-3}$	$(0.66 \pm 0.06) \cdot 10^{-3}$	0.16 ± 0.01
This (bkg subtr.)	$(4.02 \pm 0.06) \cdot 10^{-3}$	$(0.37 \pm 0.36) \cdot 10^{-3}$	0.09 ± 0.09

Table 2. Two-photon characterization of single-photon source, Poisson source and our source without and with background subtraction.

From our experimental data we obtained, with background subtraction, results for Γ_2 that are compatible with 0 as for ideal single-photon sources. We also note that $\mathcal{E}[\Gamma_1]$, is in agreement with the estimated optical losses and a previous detector calibration [38].

An alternative characterization metric for single-photon sources, was proposed by Grangier *et al.* [40]. They introduced an “anticorrelation criterion” based on the parameter $\alpha = Q(2)/[Q^{(I)}(1) Q^{(II)}(1)]$ ((I), (II) indicate the two detectors after the variable beam splitter).

For an ideal single-photon source $\alpha = 0$, while $\alpha \geq 1$ corresponds to classical sources. From our experimental data $\mathcal{E}[\alpha] = (0.18 \pm 0.02)$ and $\mathcal{E}[\alpha] = (0.11 \pm 0.11)$ with and without background subtraction, respectively, ensuring that conditional single-photon output dominates for our source.

Acknowledgments

We thank R. Alicki, E. Knill, N. Gisin, and E. Tiesinga for helpful discussions. This work has been supported in part by Regione Piemonte (E14) and by the MURI Center for Photonic Quantum Information Systems (Army Research Office (ARO)/Intelligence Advanced Research Projects Activity (IARPA) program DAAD19-03-1-0199), the IARPA entangled source programs, and European Communitys Seventh Framework Programme, ERA-NET Plus, under Grant Agreement No. 217257.